

# AUTOMATIC DETECTION OF LANDSLIDE FEATURES WITH REMOTE SENSING TECHNIQUES IN THE BETIC CORDILLERAS (GRANADA, SOUTHERN SPAIN)

T. Fernández <sup>a\*</sup>, J. Jiménez <sup>b</sup>, P. Fernández <sup>b</sup>, R. El Hamdouni <sup>b</sup>, F.J. Cardenal <sup>a</sup>, J. Delgado <sup>a</sup>, C. Irigaray <sup>b</sup>, J. Chacón <sup>b</sup>

<sup>a</sup> Department of Civil Engineering Faculty, Campus de Fuentenueva s/n, Ed. Politécnico, University of Granada, 18071 Granada- (jorgejp, pazferol, rachidej, clemente, jchacon)@ugr.es

<sup>b</sup> Dept. of Cartographic, Geodetic and Photogrammetric Engineering, Campus de las Lagunillas, Ed. Tecnología e Ingeniería, University of Jaén, 23071 Jaén- (tfernan, jcardena, jdelgado)@ujaen.es

**KEY WORDS:** Automatic Detection, Landslides, Remote Sensing, Betic Cordilleras

## ABSTRACT:

In this work we present the first results of an analysis applied to detection of landslides features using remote sensing techniques in rock masses at the Betic Cordilleras (southern Spain). After geometric and radiometric corrections, several techniques are used to facilitate a first visual approach to landslide identification, from enhancement and filtering (laplacian and textural) of panchromatic images, to colour compositions and fusions, vegetation index (NDVI) calculus and principal component analysis of multi-spectral imagery, corresponding to different sensors (Landsat ETM, Spot 5 and Ikonos). By means a GIS analysis, we compute basic statistics of whole images and pixels corresponding to different landslides typologies (rock falls, rock slides and debris flows) and in addition Kolmogorov-Smirnov coefficient to estimate the correlation between images and movements. In general terms, original panchromatic and multi-spectral bands present better correlations than processed images (filters, NDVI and PC bands), being the spectral signature different depending on landslides typology. Rock falls appear in darker zones of images while rock slides and especially debris flows appear in clearer zones. In this way, digital classification allows identify mobilized areas by typologies, but partially mixed with other land-uses such as soils, fresh rock and alluvial materials. The employment of textural filters (variance, mean euclidean distance and GLCM entropy) that present higher values in landslides zones permit the discrimination among landslides and other land-uses. The conclusion is the need of combining digital classification and textural analysis to identify landslide features or mobilized areas.

## 1. INTRODUCTION

Remote sensing techniques have been widely used from 1990 years in landslide research and for this purpose different spatial and spectral resolution imagery have been employed. This research includes photo-interpretation and inventory of large landslides, determinant factors analysis, stereoplotting of movements, and automatic detection by textural analysis.

The irregular boundaries and surface textures of landslides mean that they often produce characteristic features that can be enhanced in remote sensing imagery through textural analysis. In this sense different edge enhancement filters such as Sobel and laplacian (Eyers et al., 1995; Mason et al., 1995) have been applied to identify the hummocky main body, the accumulation toe, and the crown and back scarp of the landslides. More sophisticated statistical methods such as grey level co-occurrence and textural spectrum (Wang and He, 1990) are able to discriminate between rough and smooth surfaces and to landslide detection in different environments (Hervás and Rosin, 1996, 2001; Hervás et al, 1996, Whitworth et al., 2001, 2005). These techniques have been applied to high resolution imagery (ATM, Ikonos and Quickbird) and to medium resolution imagery (Landsat, Spot and Aster), with a less detailed features detection but with a lower noise (Hervás and Rosin, 2001). These textural analyses are usually a good approach to landslide detection, discriminating between unstable and stable zones.

Other approaches to landslide research consist in image enhancement techniques, especially colour compositions (false

colour, FCC or real colour, RCC). In this sense, different image compositions and fusions (pan-sharpening) have been made, taking advantage of the higher spectral resolution of multi-spectral imagery and the higher spatial resolution of panchromatic imagery (Nichol and Wong, 2005; Nichol et al., 2006). The best results are obtained in zones with a closed vegetation cover and affected by debris flows or debris slides, where a strong contrast between mobilized zones (with a loss of vegetation cover) and non-mobilized zones (that conserve the vegetation cover) takes place, especially in NIR band. Nevertheless, features with a similar spectral properties to landslides scarps, such as roads, ways, channels, etc. have to be eliminated through corridor filters along linear features and slope filters (Haeberling et al., 2004).

The determination of vegetation index NDVI (Chang and Liu, 2004) or other index between image bands such as NDMIDIR (Vohora & Donohue, 2004; Zhang et al., 2005) between near and middle infrared and the analysis of spectral signatures produce similar results that false color compositions. In this way, the NDVI index has been very useful to identify debris flows in zones with a dense vegetation cover. Principal components analysis (PCA) has also been used to intervene in classifications (Whitworth et al., 2005) and in visual interpretation by means of false colour compositions.

3D and stereoscopic analyses allow a good interpretation of landslides through recognition of morphological features such as scarps, accumulation zones, etc., not easily identifiable in 2D views. From 3D image views over a DTM (Hervás and Rosin,

\* Corresponding author: Tomás Fernández (tfernan@ujaen.es) University of Jaén, Spain.

2001; Haeberling et al., 2004) to photogrammetric techniques such as stereoscopic viewing or DTM extraction (Zhihua, 2005; Weirich and Blesius, 2006), these methodologies have been used in landslides studies when data are available. Finally, multi-temporal imagery has been used to study landslide activity from pixel change detection techniques (Rosin and Hervás, 2003) to quantitative 3D analysis of landslides displacement.

**2. STUDY AREA AND IMAGE DATA**

This is an area prone to terrain instability, because of a combination of an abrupt relief and a geological setting with a high susceptibility to landslides.



Figure 1. Geographical location.

**2.1 Geographical location and relief description**

The study area is located in a region of about 600 Km<sup>2</sup>, located in Granada province (Southern Spain) at the South of Sierra Nevada, between this range and the coast of Mediterranean Sea. This is a rural area with small villages disseminated overall the region and communicated by secondary roads. The relief is abrupt with a vertical interval near 3000 meters with steep slopes. Drainage network is very dense and organized, with a lot of ravines tributaries of Guadalfeo River.

**2.2 Geology, climate and vegetation**

From the geological point of view, the area is located within Internal Zones of Betic Cordilleras, between Alpujárride and Nevado-Filabride Domains. Alpujárride Domain is formed by metapelitic and carbonate rock masses, while Nevado-Filabride Domain is formed mainly by metapelitic rock masses. In between them, Neogene and Quaternary materials (conglomerate, sands clays and marls) outcrop.

The climate is typically Mediterranean except in higher zones over 1800 meters. Mean temperatures vary from 12°C in winter to 18°C in summer. Annual mean precipitation is about 600-800 mm, but in an irregular regime with wet years over 1000 mm and dry years below 500 mm. Vegetation is variable with zones well vegetated (pine and oak forests, dense brush, grass) and arid zones with scarce vegetation (brush and waste lands).

**2.3 Image data**

High to medium resolution remote sensing imagery from different satellites in panchromatic and multi-spectral modes have been used. Images properties are summarized in table 1. Spot 5 and Landsat ETM+ images cover the whole zone while Ikonos is available only in the central sector. In Figure 1 we also show the distribution of satellite images.

Satellite/ Sensor	Bands	Resolution		
		Spa	Band	Rad.
Ikonos	Panchromatic	1	1	2048
	Vis(RGB)-NIR	4	4	2048
Spot 5	Panchromatic	2,5	1	256
	Vis(GB)-NIR	10	3	256
	SWIR	20	1	256
Landsat 7 ETM +	Panchromatic	15	1	256
	Vis(RGB)-NIR- SWIR	30	6	256
	TIR	60	1	256

Table 1. Images properties. Vis: Visible; R: Red; G: Green; B: Blue; NIR: Near Infrared; SWIR: Short-wave (middle) Infrared; TIR: Thermal Infrared

**3. IMAGE PROCESSING**

Image processing employed in this work includes several techniques, from image pre-processing to digital classification that can be seen in figure 2.

**3.1 Pre-processing**

Here, we talk about techniques to converting original images to cartographic products and to preparing image to other analysis. First, images have been geometrically corrected and georeferenced in the UTM projection. Correction has been made by means control points and models implemented in ERDAS software for different sensors (Ikonos, Spot, etc.), over a DTM of 10 m resolution. Second, we have applied single Chavez radiometric correction to eliminate atmospheric effects.

**3.2 Enhancement and colour compositions**

After pre-processing, image bands are enhanced by means of lineal stretch of histograms (figure 2 c), except in Ikonos images where square-root and logarithmic stretch are also applied. The available Ikonos images have wide shaded zones and in this case this non-lineal stretch are recommended (Roberts, 2005).

Different colour compositions have been made from corrected image bands. Apart from RCC, FCC with inclusion of NIR band allow to distinguish between zones covered or non-covered by vegetation, a factor which can show the presence of landslide scarps. Other colour compositions with inclusion of SWIR are useful to show lithological changes or boundaries, frequently related to landslides.

Finally, in those image compositions where Visible and NIR bands intervene, fusion of multi-spectral and panchromatic (that cover VNIR spectrum region) images have been made. These fusion or pan-sharpening techniques provide both RCC and FCC with the higher spatial resolution of panchromatic images (Nichol and Wang, 2005).

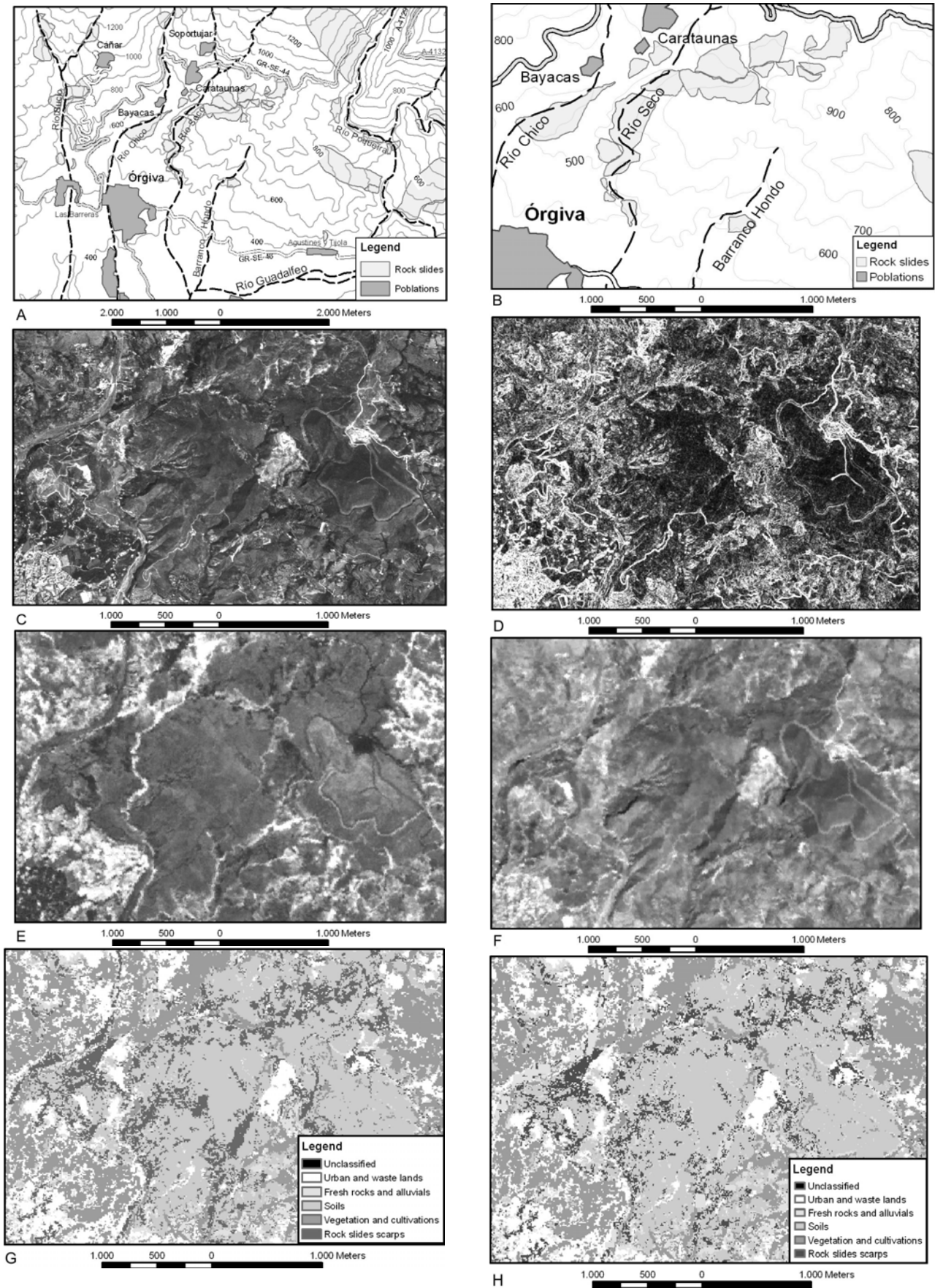


Figure 2. Spot 5 Image: A. Location; C: Panchromatic corrected image; E: NDVI vegetation index; G: Supervised classification.

Figure 2. B. Rock slides location; D: Variance texture filter; F: PC band 1; H: Modified supervised classification.

### 3.3 Filters

Different filters have been applied mainly to panchromatic images. First, we use convolution edge-enhancement filters (3x3) such as laplacian and Sobel to find landslides lineal features: scarps, crown, limits, etc. Second, we apply textural filters such as variance (figure 2 d), mean euclidean distance (MEUC) and grey-level co-occurrence matrix (GLCM) entropy to calculate the variability of one pixel to its neighbourhoods. Nevertheless, these textural filters, especially when they are applied to thermal bands allow detect irregular morphologies as those in landslides (Whitworth et al., 2003, 2005).

### 3.4 Indexes and transformations

Vegetation indexes are very useful to identify landslide and debris flow scarps, especially in zones with a dense vegetation cover (Chang an Liu, 2004). Besides, they decrease the differences between shaded and sunned areas, as those we can find in Ikonos images of the study zone (figure 2 e).

PCA allow transform original (corrected) image bands in new uncorrelated bands. By this reason, single bands and FCC elaborated from PCA show a higher variability than original bands and allow detect features more clearly. In this study, we have obtained a number of PC bands equal to original bands. In figure 2 f, PC 1 band is shown.

### 3.5 Digital classification

Digital supervised classification has been made from multi-spectral imagery (figure 2 g-h), discriminating between four basic land-uses and materials: urbanised-waste lands, vegetation (from grass to cultivations to forest), soils-brush cover, and fresh rock masses-alluvial deposits. Apart of these, landslides in their different typologies have been established as fifth class. In this way, three classified images for each sensor have been elaborated. An analysis of separability of spectral signatures will be done to decide if it is possible to distinguish between landslide typologies and between landslides and stable terrain.

## 4. GIS ANALYSIS

Two approaches have been made: first, visual interpretation from enhanced images, filters, colour compositions and classifications (figure 2); second, a GIS statistical analysis.

### 4.1 Zone statistical analysis

In this analysis, a frequency distribution or histogram of an image in the zone defined by other image o vector feature is obtained. In our case, we determine the histogram of the different image bands in a pixel sample of different typologies of landslides (rock falls, rockslides and debris flows) and compare this with the histogram of whole image.

### 4.2 Correlation coefficients

To determine if an image can be useful to discriminate between landslides and stable zones Kolmogorov-Smirnov coefficient (KS) is calculated. This coefficient shows the differences between whole image histogram and landslide samples histograms. KS coefficient is higher as the difference between histograms or distributions. Results are shown in table 2.

Sensor	Image		Rock falls			Slides			Debris flows		
	Me	St	Me	St	KS	Me	St	K	Me	St	KS
Ikonos Pan	25	13	18	13	-28	26	14	04	23	15	-14
Laplacian	41	24	42	23	03	41	25	02	41	24	02
Variance	117	26	106	34	-21	120	27	07	115	33	-10
Mean Eu.	35	12	31	14	-18	37	12	06	35	14	-08
GLCM E.	139	60	128	58	-17	145	56	06	146	56	07
M-Blue	10	6	8	5	-24	12	7	07	11	8	10
M-Green	17	10	13	10	-27	19	12	06	18	13	-10
M-Red	17	11	13	12	-28	19	13	05	18	14	-11
M-NIR	35	19	24	18	-27	37	20	04	32	21	-13
NDVI	171	22	166	22	-12	168	21	-05	164	23	-14
PC-1	30	15	21	16	-27	32	17	05	29	19	-12
PC-2	178	11	176	8	-18	177	12	-08	175	11	-17
PC-3	155	5	154	5	-18	154	5	-13	154	5	-11
PC-4	119	4	120	3	12	119	4	04	119	4	03
Classific.	-	-	-	-	22	-	-	19	-	-	13
Final im.	-	-	-	-	25	-	-	25	-	-	18
Spot 5 Pan	31	10	27	8	-20	32	9	08	30	9	-04
Laplacian	40	23	40	21	02	40	26	02	40	25	02
Variance	135	47	131	47	-07	139	47	07	139	47	08
Mean Euc.	57	24	53	24	-06	60	23	06	60	23	07
GLCM E.	142	60	132	61	-07	151	58	06	153	56	07
M-Green	29	8	27	7	-13	31	8	11	30	8	04
M-Red	35	11	30	9	-19	35	10	07	34	10	-03
M-NIR	50	11	42	11	-26	48	12	-10	47	11	-11
M-SWIR	42	9	37	8	-23	42	8	04	41	9	-8
NDVI	118	32	115	24	-10	112	30	-11	112	26	-08
PC-1	76	17	67	16	-22	77	15	05	74	17	-05
PC-2	21	9	17	7	-19	19	10	-19	19	8	-15
PC-3	0	1	0	1	-04	0	1	-02	0	1	-02
PC-4	5	1	5	1	22	5	1	23	5	1	17
Classific.	-	-	-	-	38	-	-	25	-	-	26
Final im.	-	-	-	-	42	-	-	31	-	-	34
LSat-Pan	56	12	51	12	-21	58	12	05	55	13	-09
Laplacian	42	24	42	23	02	43	25	03	42	25	02
Variance	141	28	149	30	13	148	26	11	152	30	17
Mean Euc.	75	43	87	48	13	84	46	10	91	51	15
GLCM E.	186	57	201	47	11	199	50	10	205	48	16
M-Blue	50	12	48	9	-09	51	10	11	50	11	02
M-Green	54	14	50	13	-14	56	12	07	54	14	-02
M-Red	69	23	62	21	-17	70	20	05	68	23	-04
M-NIR	66	13	58	11	-25	67	16	10	63	15	-11
M-SW1	101	25	92	27	-17	101	23	-03	97	27	-08
M-SW2	70	20	66	22	-14	69	18	-03	68	21	-05
NDVI	101	31	100	21	10	99	30	-04	100	28	-03
PC-1	166	39	153	43	-18	167	36	04	161	43	-06
PC-2	18	12	15	9	-12	16	12	-09	15	11	-11
PC-3	0	0	0	0	0	0	0	0	0	0	0
PC-4	22	5	23	3	14	24	5	12	23	4	09
Classific.	-	-	-	-	15	-	-	8	-	-	7
Final im.	-	-	-	-	16	-	-	10	-	-	11

Table 2. Statistical analysis: Me: Mean; St: Standard deviation; KS: Kolmogorov-Smirnov coefficient (normalized to 100).

## 5. RESULTS

From the statistics of table 2 and visual interpretation of enhanced images and colour compositions, we can conclude that, in absolute terms, values of KS coefficient are low in all the cases although, in relative terms, some remarks can be outlined.

First, rock falls are the typology that shows higher radiometric differences regarding to the whole image, generally with lower DN values in rock falls scarps (darker) than the whole image. These differences can be observed in panchromatic and multi-

spectral images, as in derivatives (filters, NDVI and PC bands), although differences are higher in original corrected and enhanced images. Filters and NDVI present DN values lower (darker) in rock falls sample than the whole image and a more irregular behaviour of PC images. By sensors, the best results can be observed in Ikonos, while in this case, Spot 5 y Landsat 7 show similar results.

Rock slides have very poor correlations (near to 0) in most of cases. Usually, DN values of rock slides sample are relatively higher (clearer) than the whole image in panchromatic image, its filters, the visible bands and some PC bands. However, NIR band, NDVI and some PC bands show lower values than the whole image.

Debris flows present the more irregular results. Regarding to panchromatic image, values are clearly lower than the whole image in Ikonos, but it become similar in images corresponding to Spot 5. On his hand, filters corresponding to Landsat image present higher values in debris flows zones than in the whole image. Regarding to multi-spectral image, most of bands present DN values lower in landslides sample, but in some visible bands can become higher. However, NIR band and NDVI always appear in debris flows with lower DN values than whole image.

Finally, in all the movements, KS coefficients calculated in classified images are higher that those obtained in original and derivative bands.

## 6. DISCUSSION

In spite of low Kolmogorov-Smirnov coefficient, the results of GIS analysis allow extract the following observations, regarding enhanced original, filtering and classification images.

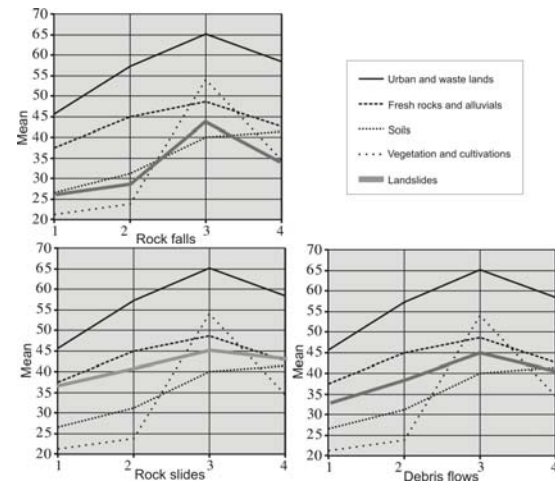
Starting by original images, rock falls are strongly related to shaded zones in the study area, and because of it, they present lower DN values than the whole image. The higher correlations are found in Ikonos image, taken in winter and with a higher extension of shaded zones, associated frequently with rock falls. This is a local fact, because in this area rock falls are located in the northern slopes of Sierra de Lújar. In other zones, with rock falls in cliffs oriented to South (in northern hemisphere, of course), rock falls can be associated with relative higher DN values, as the other landslides do.

Rock slides scarps are zones that appear clearer in the image because fresh rock (that outcrop in this zones) generally present a higher reflectance in visible bands than the surrounding soil and vegetation cover do. The lower values of KS coefficient are probably due to the use of the whole movement and not only the scarp in the cross correlation.

Debris flows have complex relationships with reflectance and DN, depending on the soil illumination, due to these movements are located in ravines o steep slopes that can be affected irregularly by shades. By that reason, debris flows present lower KS coefficient values, not because they present similar values than surrounding terrain but they appear with DN values higher than the whole image (sunny zones) or with DN values lower than the whole image (shaded zones). Since images from different sensors are taken in different months, these images present different DN values and KS coefficients.

Laplacian filter, as an edge-enhancement filter, highlights linear elements and borders, and can be used for delimitate movements, but DN values do not show significative differences regarding original image. Use of textural filters results more interesting in this case, because they produce higher differences between zones of movements and the whole image. In this case the image resolution and observation conditions become very important. In Landsat images, filters present higher DN values in mobilized zones, no matter the typology; in Ikonos slides present also higher values but rock falls and debris flows present lower values than the whole image; and finally, in Spot images DN values of mobilized zones are similar than the whole image.

Regarding supervised classifications, in figure 3 we show the spectral signatures corresponding to the three classifications determined here. Difficulties to distinguish between landslides and some land-uses can be observed. Rock falls appear very similar to soils, rock slides is only a little darker than soils, and debris flows are very close to fresh rock and alluvial materials.



To discriminate between the different landslide typology and other land-uses we can use textural filters, specifically variance that shows the best correlations with landslides. In this way, zones of rock slides present higher values of variance than soils do, and debris flows present values of variance clearly higher than fresh rock and alluvial materials do. In both cases, a single matrix approach between classifications and variance filter permits to modify the classification to obtain a final image in which these landslides typologies appear more clearly separate from other land-uses. Zones previously classified (wrongly) as landslides pass to soil or fresh rock, so correlation coefficients (of final classification) increase (table 2).

Results of different sensor present some differences between mean DN values and KS coefficients. In general, the best final results are found in Spot images, following by Ikonos and Landsat. Perhaps, the presence of important shaded zones in Ikonos make the results worse regarding to Spot (image from summer, free of shades). However, results of filtering are generally better in Landsat, probably because pixel size of other images is enough small to detect textures in a 3x3 window.

Finally, a post-processing image will be necessary to eliminate some elements as roads, waste mining, quarries, etc. These are elements clearly identifiable and consequently eliminable. To this purpose, corridors along linear or polygonal elements and slope filters can be used (Haerberling et al., 2004).

## 7. CONCLUSIONS

There are many published approaches to the study of landslides by means remote sensing. Depending on the characteristics of study zone and the available images, the approaches may be different but all of them are based in multi-spectral information (band compositions, indexes, PCA and digital classification) and texture analysis (filtering and image segmentation).

In this study both approaches are combined by means digital classification and texture filters (variance). Previously, statistical and cross-analysis allow establish relative correlation between landslide inventories and images, and also recognize intervals and average DN values in which landslides occur, regarding to different images. In this way rock falls are related to lower values (darker zones) of original enhanced images while slides and debris flows are related to higher values (clearer zones).

Digital classification from multi-spectral analysis has established a class for each type of landslide but with a certain mixture with other classes such as soils, fresh rock and alluvial materials. In this point textural analysis can solve the uncertainties, discriminating landslide classes from other land-uses and making more accuracy the classification.

Finally, the usability of remote sensing techniques in these studies has been probed once more again, and future research will be related with advances in enhancement of images (to solve problems with shades and illumination), in textural analysis (segmentation) and in combining these techniques with photogrammetry and field work at larger scales.

## REFERENCES

Chacon, J.; Irigaray, C., Fernández, T.; El Hamdouni, R., 2007. Engineering geology maps: landslides and geographical information systems. *Bull. Eng. Geol. & Env.*, 65, 341-411.

Chang, R.T. & Liu, J.K., 2004. Landslide features interpreted by neural network method using high-resolution satellite image and digital topographic data. *Proc. ISPRS04, Istanbul, Turkey*.

Eyers, R., Moore, J. McM., Hervás, J. and Lui, J. G., 1995. Landslide mapping using digital imagery: a case history from south east Spain". *Proc. 31st Annual Conf. on Geohazards and Engineering Geology*, 379 – 388. 1995, Coventry, UK

Haerberlin, Y.; Turberg, P.; Retière, A.; Senegas, O. & Parriaux, A. (2004). Validation of SPOT-5 satellite imagery for geological hazard identification and risk assessment for landslides, mud and debris flows in Matagalpa. *Proc. ISPRS04, Istanbul, Turkey*.

Mason, P. J., Rosenbaum, M. S. and Moore, J. McM. "Texture analysis using multi-temporal digital data for landslide hazard mapping". *Proc. 31st Annual Conference on Geohazards and Engineering Geology*, 215 – 224, Coventry, UK

Hervás, J. and Rosin, P. L. "Landslide mapping by textural analysis of ATM data". *Proceedings Eleventh Thematic Conference Applied Geologic Remote Sensing*. 395 – 402.

Hervás, J.; Rosin, P.L.; Fernández-Renau, A.; Gómez, J.A. and León, C. 1996). Use of airborne multispectral imagery for

mapping landslides in Los Vélez district (south-eastern Spain). In Chacón, J., Irigaray, C. and Fernández, T.(1996) (Eds.) *Landslides*. Pp. 353-362. Ed.Balkema. Netherlands.

Hervás, J. y Rosin, P.L. (2001). Tratamiento digital de imágenes de teledetección en el espectro óptico para el reconocimiento y control de deslizamientos. *V Simposio Nacional de Laderas y Taludes Inestables*.

Metternicht, G.; Hurni, L. & Gogu, R. (2005). Remote sensing of landslides: An analysis of the potential contribution to geo-spatial systems for hazard assessment in mountainous environments. *Remote Sensing of Environment*, 98, 284 – 303.

Nichol, J & Wong, M.S. (2005). Satellite remote sensing for detailed landslide. Inventories using change detection and image fusion. *Intern. Journal of Remote Sensing*, 26, 9, 1913–1926.

Nichol, J.; Shaker, A. & Wong, M.S. (2006). Application of high-resolution stereo satellite images to detailed landslide hazard assessment. *Geomorphology* 76, 68– 75

Roessner, S.; Hans-Ulrich Wetzel, W.; Kaufmann, H. & Sarnagoev, A. (2005). Potential of Satellite Remote Sensing and GIS for Landslide Hazard Assessment in Southern Kyrgyzstan (Central Asia). *Natural Hazards*, 35: 395–416.

Rosin, P.L. and Hervás, J. (2005). Remote sensing image thresholding methods to determining landslide activity. *International Journal of Remote Sensing*, 26, 6, 1075-1092.

Vohora, V.K. and Donohue, S.L. 2004. Application of remote sensing data to landslide mapping in Hong Kong. *Proc. ISPRS04, Istanbul, Turkey*

Wang, L. and He, D. C. "A new statistical approach for texture analysis". *Photogrammetric Engineering and Remote Sensing*, 56 (1), 61 – 66. 1990.

Weirich, F. and Blesius, L. (2006). Comparison of satellite and air photo based landslide susceptibility maps. *Geomorphology*, 87, 352-364. Elsevier, UK.

Whitworth, M., Giles, D., Murphy, W., 2001. Identification of landslides in clay terrains using Airborne Thematic Mapper (ATM) multispectral imagery. *Proc. 8th Intern. Symp. Remote Sensing. SPIE Volume 4545*, 216 – 224.

Whitworth, M. C. Z.; Giles, D. P. & Murphy, W. (2005) Airborne remote sensing for landslide hazard assessment: a case study on the Jurassic escarpment slopes of Worcestershire, United Kingdom. *Quarterly Journal of Engineering Geology and Hydrogeology*, 38(3), 285 - 300.

Zhang, Z.; Gong, H.; Zhao, W.; Zhang, Y. 2005. Application of remote sensing to study of landslides. *IEEE*, 1546-1549.

## ACKNOWLEDGEMENTS

This research was funded by CYCIT project CGL2005-03332 (BTE), project P06-RNM-02125 funded by the Andalusian Research Plan, and Research Groups TEP-213 and RNM 221 of Andalusian Research Plan.